Electrical Power and Energy Systems 94 (2018) 77–87

Contents lists available at ScienceDirect

Electrical Power and Energy Systems

journal homepage: www.elsevier.com/locate/ijepes

Analysis and prediction of vulnerability in smart power transmission system: A geometrical approach ☆

Sudha Gupta *, Faruk Kazi, Sushama Wagh, Navdeep Singh

Electrical Engineering Department, Veermata Jijabai Technological Institute (V.J.T.I.), Mumbai 400 019, India

ARTICLE INFO

Article history:
Received 31 July 2016
Received in revised form 24 February 2017
Accepted 23 June 2017

Keywords:
Cascade link failure
Effective resistance
Gaussian distribution
Graph centrality
Laplacian Pseudo Inverse (LPI)
Power Flow Index (PFI)
Transmission line system
Vulnerability Index (VI)
Wide Area Monitoring Systems (WAMS)

ABSTRACT

The paper proposes a novel methodology to analyze and measure the impact of line tripping on grid vulnerability which may lead to cascade failure in smart power transmission system. The key contributions are analysis of current flow path and identification of critical line from normal to perturbed grid with the knowledge of grid topology. To achieve this two performance indices i.e. power flow index and vulnerability index have been defined on the bases of geometry of current flow path. A power flow index is defined to analyze impact of topological changes on current flow path and identify underloaded and overloaded lines. Probability of the critical line and the location of vulnerability center are identified by the vulnerability index. Analytically defined performance indices are applied analyzed and validate using the benchmark IEEE 30 bus power system. The critical line identified by proposed indices is also verified with the probabilistic framework. The proposed methodology allows to focus attention on the power grid vulnerable areas and can help the control system operator to investigate the changes in power flow on transmission lines and initiate the necessary corrective action. The methodology proposed in this paper can be used in security assessment and centralized monitoring of power flow in future smart grid wide area monitoring protection and control system.

1. Introduction

Power system is a complex interconnected network. It is an integration of green energy and communication technology with power system that has made the grid smart. At the same time, growth in generation and demand without network expansion further increases the complexity of power network and creates various security issues. It may disturb security margin and create unplanned line outage that may lead to cascade failure. Cascade failure due to line loading in power transmission system is one of the prime issues [1–3]. Cascade modelling using time dependent phenomena in [4], showed that sympathetic tripping and weather conditions have the most significant impact on the load interruption costs and it depends on the operating scenarios under consideration.

In literature, researchers have applied considerable efforts in analysis and understanding of cascade failures in power networks. Among such efforts, deterministic, probabilistic and topological models have been used widely. In the deterministic (N-1) security model, (N-1) checking and contingency ranking methods [5–7] are used commonly to carry out the overloaded line or bus for successive line tripping. Power grid is a huge and complicated interconnected network where tracing of any uncertainty by checking each and every line is a very tedious task. Probabilistic and topological models to power flow analysis is computationally less complex compared to deterministic model. These models replace detailed analysis of the power system equations and provides additional insights such as higher order moments in probabilistic approach [8,9] and spectral analysis of current flow path in the topological approach [10–13] which allows to focus attention on the power grid vulnerable areas. Analysis and prediction of grid vulnerable area is now becoming more feasible with the advancement in WAMS, [14,15] such as online, GPS time tag PMU data. Availability of online PMU data from WAMS helped in making simulation based modelling to data centric modelling.

Disturbances in power transmission system increase with increase in complexity such as integration of green energy in smart power system. To reduce computational complexity and increase the security of smart power transmission system, two performance index based on grid geometry has been proposed in this paper. It captures the geometry of load flow path, analyze and measure

☆ This work was supported by the Center of Excellence in Complex and Nonlinear Dynamical Systems, Veermata Jijabai Technological Institute, Mumbai, India, under TEQIP-II subcomponent (1.2.1).

* Corresponding author at: Electronics Engineering Department, K.J.S.C.E., Mumbai, India.
E-mail address: sudhagupta@somaiya.edu (S. Gupta).

http://dx.doi.org/10.1016/j.ijepes.2017.06.033
0142-0615/

the effect of topological changes on load flow path and identify the critical line in the perturbed grid. With the use of proposed methodology, an operator at the central monitoring system can visualize the effect of line tripping on vulnerability in transmission system and can identify where the bottleneck lies in the network, thereby taking the corrective action well in advance. Early prediction of critical link may prevent the onset of blackouts by initiating remedial action such as load shedding, load balancing or controlled islanding [16–18] before it affects the entire power network.

The rest of the paper is organized as follows: Section 2 explains the topology of power network. Geometry of current flow path has been introduced in Section 3 along with the concept of auxiliary grid. Section 4 presents the proposed methodology and formulation of PFI and VI metrics. Section 5 presents a case study to validate the proposed methodology using the benchmark IEEE 30 bus system. Some open research issues are discussed in Section 6 along with conclusions.

2. Topology of power network

A model of a transmission line of power network is shown in Fig. 1. Where, $|V_i|, |V_j|$ is respective voltage magnitude at bus i and j. p_i and p_j are injected active power, Z_{ij} is an impedance of the transmission line connecting to bus i and j. δ_i and δ_j are voltage phase angle at bus i and j respectively. For DC power flow the voltage magnitude at all buses is maintained at 1 per unit (pu). Further, as the system synchronization is always maintained under normal operating conditions the angular difference between two neighboring nodes is very small. Hence, active power on transmission line expressed as

$$p_{ij} = \frac{(\delta_i - \delta_j)}{Z_{ij}} \tag{1}$$

Power flow on transmission lines is varying as per supply and demand with time. A slight change in grid parameters will change power flow on transmission line. Hence traditional contingency analysis using AC or DC load flow equations [19] is a complex and tedious task. This issue can be handled by the topological framework of power grid wherein load flow can be analyzed on the bases of changes in physical topology between buses and transmission lines.

Physical topology of a power grid maps a complex power network in a graph G by converting generators and substations as a node and transmission lines and transformers as a link with line impedance as a path length. This physical topology gives undirected and sparsely connected graph G and is represented by (2).

$$G = (V, E, Z) \tag{2}$$

where V is a set of nodes or vertices (buses), $V = (v_1, v_2, \ldots, v_N)$ and E is a set of edges (transmission lines) $E = (e_1, e_2, \ldots, e_M)$ of G. The weight of the corresponding line i.e. Z_{ij}, is the line impedance between nodes v_i and v_j.

A spectral graph theory inter connectivity between nodes and links and can be described by the graph Laplacian (L_G) matrix [20]. Consider the weighted adjacency matrix (A_{ij}) of size $N \times N$ symmetric matrix, where N is the total number of vertices and ij is the ith row and jth column of elements $(i = j = 1, \ldots, N)$ of the matrix. The A_{ij} in (3) represents physical topology of a network which defines adjacent vertex connectivity in a graph. For an undirected graph,

$$A_{ij} = A_{ji} = Z_{ij} \begin{cases} \text{for}, & v_i v_j \in V \\ \text{otherwise}, & 0 \end{cases} \tag{3}$$

The diagonal matrix $D_{ii}, (j = i)$, contains the weight of vertex v_{ii}

$$D_G = D_{ii} = \sum_{j=1}^{N} Z_{ij} \tag{4}$$

To understand the geometry of power network the graph Laplacian (L_G) matrix is defined from (3) and (4). The L_G matrix is known to be symmetric and positive semidefinite [20], and its real eigenvalue defines graph connectivity.

$$L_G = D_G - A_{ij} \tag{5}$$

$$L_G = L_{ij} \begin{cases} \text{if } i \neq j \text{ and } (i,j) \in V, & -Z_{ij} \\ \text{if } i = j, & D_G \\ \text{otherwise}, & 0 \end{cases} \tag{6}$$

The weighted L_G matrix (6) has all the off-diagonal entries non positive and diagonal entries non negative. The sum of matrix elements in each row is zero. Hence, L_G is a positive semidefinite singular matrix [20] which defines graph connectivity. Authors of [16] used algebraic connectivity (eigenvalues) of L_G matrix for sequential islanding of power system in order to provide security strategy.

3. Geometry of current flow path

The issues before applying the geometrical approach to power grid is that the power network should be expressed by such a simple way as the rate of commodities passing through a node or link. However, electrical power requires two variables to be identified, a generalized coordinate (charge) and a generalized force (voltage). Another challenge is that the electrical power, flows along all transmission lines from generating source to consuming loads according to power flow equations. To analyze power flow on transmission line by geometry of current flow path, it is important to describe physical topology (line and node connectivity) in terms of electrical topology (resistive paths between pair of vertices). These issues are addressed and solved in the literature [5,13], by introducing the concept of Auxiliary Grid (AG).

3.1. Concept of auxiliary grid

To employ the geometrical concept in the power flow problems, physical topology of power network is transformed into electrical topology with the help of spectral graph theory and named as auxiliary grid (AG). PG to AG transformation carried in such a way that the geometry of power flow in the power grid can be concluded from the geometry of resistive path difference in AG. To achieve this physical topology of power grid is defined graphically by (L_G) (6). In graph theory for computation of grid connectivity, state of the art Jacobian methodology is used. However, this methodology compute only few eigenvalues of L_G matrix which do not provide any insight into the individual path lengths between pair of vertices. To obtain better insights of grid connectivity and explore hidden geometry of path between pair of vertices v_i, v_j the L_G matrix transforms into AG by using Laplacian pseudo inverse (LPI) transformation (Fig. 2). Isomorphism (same number of vertices, edges, and also the same edge connectivity) between PG to AG is established by LPI kernel. The LPI is inverse of L_G which is defined here as L^+ matrix, where each matrix element is represented as

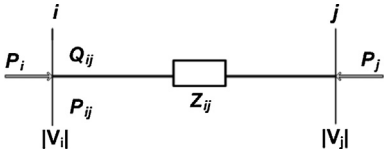

Fig. 1. Power grid transmission line model.

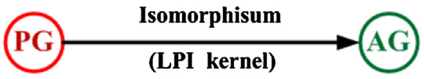

Fig. 2. Concept of auxiliary grid.

coordinate point (v_i, v_j). The LPI, (L^+) and its matrix elements (line impedance) explores an n dimensional Euclidean embedding [20] across the line in AG. L_G as well LPI is a connected graph, where vertices are connected through line impedance hence LPI matrix can be conveyed in terms of resistance matrix, auxiliary resistive grid or AG wherein connectivity between vertices defines electrical topology of AG.

An electrical topology of AG is defined from the L_0^+ matrix. L_0^+ matrix is a sub matrix of L^+ in AG, where the rows and column of reference vertex v_0 considered as zero (Ground). A grid is connected to a reference vertex v_0, if there is a path from every node in the grid to at least one of the reference nodes in v_0. Whenever an effective resistance exists between a pair of vertices and if any of the vertex connected to the reference vertex (ground), a current will flow in the AG. Hence L_0^+ is also called as grounded LPI [13,22] or Kirchoff's matrix. Consider a six vertices and seven edge network system. The physical topology and the electrical topology of the same are shown in Figs. 3 and 4. The physical topology of PG provides the information of nodes and links connectivity whereas electrical topology of a network manages the current flow path between pair of vertices in AG. Based on (3)–(6) the L_G is defined as It is well known that any complex matrix admits a unique pseudo inverse [20]. The generalized inverse (L_{ij}^+) of L_G matrix of a connected graph (8) is a real and symmetric. The grounded Laplacian inverse or Kirchoff's matrix is given in (9).

$$L_G = \begin{bmatrix} e_{1,1} & -e_{1,2} & -e_{1,3} & 0 & 0 & 0 \\ 0 & e_{2,2} & -e_{2,3} & -e_{2,4} & 0 & 0 \\ -e_{3,1} & -e_{3,2} & e_{3,3} & -e_{3,4} & 0 & 0 \\ 0 & -e_{4,2} & -e_{4,3} & e_{4,4} & -e_{4,5} & 0 \\ 0 & 0 & 0 & -e_{5,4} & e_{5,5} & -e_{5,6} \\ 0 & 0 & 0 & 0 & -e_{6,5} & e_{6,6} \end{bmatrix} \tag{7}$$

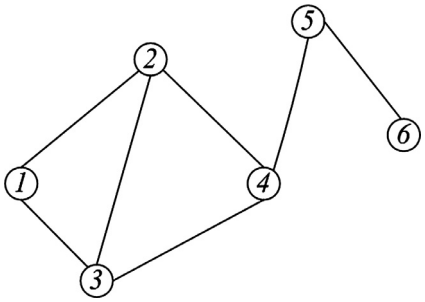

Fig. 3. Physical topology in PG.

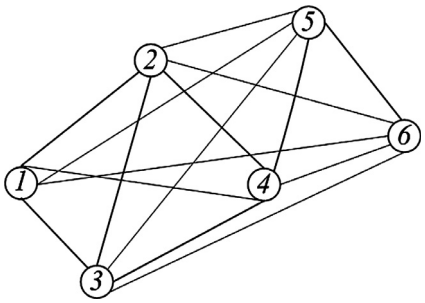

Fig. 4. Electrical topology in AG.

$$L_{ij}^+ = \begin{bmatrix} e_{1,1} & -e_{1,2} & e_{1,3} & -e_{1,4} & e_{1,5} & -e_{1,6} \\ e_{2,1} & e_{2,2} & e_{2,3} & -e_{2,4} & e_{2,5} & -e_{2,6} \\ e_{3,1} & e_{3,2} & e_{3,3} & -e_{3,4} & -e_{3,5} & -e_{3,6} \\ -e_{4,1} & -e_{4,2} & -e_{4,3} & e_{4,4} & e_{4,5} & -e_{4,6} \\ -e_{5,1} & -e_{5,2} & -e_{5,3} & -e_{5,4} & -e_{5,5} & -e_{5,6} \\ -e_{6,1} & -e_{6,2} & -e_{6,3} & -e_{6,4} & -e_{6,5} & e_{6,6} \end{bmatrix} \tag{8}$$

$$L_0^+ = \begin{bmatrix} 0 & 0 & 0 & 0 & 0 & 0 \\ 0 & e_{2,2} & e_{2,3} & -e_{2,4} & e_{2,5} & -e_{2,6} \\ 0 & e_{3,2} & e_{3,3} & -e_{3,4} & -e_{3,5} & -e_{3,6} \\ 0 & -e_{4,2} & -e_{4,3} & e_{4,4} & e_{4,5} & -e_{4,6} \\ 0 & -e_{5,2} & -e_{5,3} & -e_{5,4} & -e_{5,5} & -e_{5,6} \\ 0 & -e_{6,2} & -e_{6,3} & -e_{6,4} & -e_{6,5} & e_{6,6} \end{bmatrix} \tag{9}$$

As shown in Fig. 4, the geometry of the current flow path can be analyze with electrical topology of AG. Any topological changes in PG will change the electrical topology and geometry of current flow path in AG. Hence, power flow in PG can be estimated with current flow path in AG. It is now possible to capture the geometry of the complex power network from AG in terms of distance metric i.e. effective path distance or effective resistance (R_{eff}) and euclidean distance between pair of vertices. In the proposed methodology changes in power flow on transmission lines due to line tripping is analyze by observing the changes in R_{eff} between a pair of vertices in AG or geometry of current flow path. In a dynamic network, electric current flows through multiple paths. This excludes the presence of a distinct path or existence of the path between pair of vertices in the network. The concept of equivalent or effective resistance makes it possible to determine a distinct current flow path between pair of nodes by conceptually replacing the multiple paths between pair of vertices with a single equivalent path i.e. R_{eff}.

3.2. Effective resistance (R_{eff})

In the literature R_{eff} played an important role in distributed control and estimation problems with many applications [13,22,23]. In a connected graph, R_{eff} as shown in Fig. 5 is defined as an equivalent resistance between a pair of vertices v_i and v_j. According to Kirchoff's law at a node current entering into the node is equal to the current leaving into the node. The R_{eff} between any pair of nodes v_i and v_j is computed as;

$$R_{\text{eff}}(v_i, v_j) = (L_o^+)_{ii} + (L_o^+)_{jj} - (L_o^+)_{ij} - (L_o^+)_{ji} \tag{10}$$

where ii and jj are diagonal elements (node impedance corresponds to reference node) and ij, and ji are off diagonal elements (line impedance) of the L_0^+ matrix (7). Eq. (10) defines electrical closeness of two vertices. As PG and AG are undirected graphs hence, for $ij = ji, R_{eff(ij)}$ defined as

$$R_{\text{eff}}(v_i, v_j) = (L_o^+)_{ii} + (L_o^+)_{jj} - 2(L_o^+)_{ij} \tag{11}$$

The R_{eff} (11) between pair of vertices providing geometry of an electric path length in the AG, which will be useful for the local information of network connectivity and current flow path. R_{eff} will be small when there are parallel paths between pair of vertices.

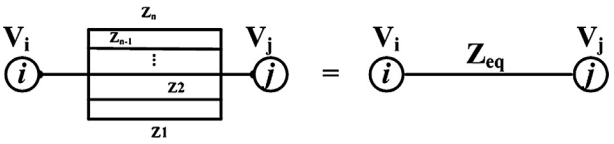

Fig. 5. Effective resistance between pair of vertices.

Any topological changes in PG, such as line tripping will change the matrix elements of L_0^+ and hence R_{eff} will change. This will change electrical topology (current flow path) between a pair of vertices in AG. Line tripping in PG directly impact on the current flow path or network geometry in AG. Hence, variation of power flow on transmission lines in PG can be analyzed by computing the current flow paths in AG.

Current flow across pair of vertices in AG obeys the fundamental Kirchoff laws. Any topological changes will redistribute the current among all existing path wherein current flow through all available paths. However, maximum current flow through the shortest path. Hence, for analysis of impact of line tripping on changes in current flow path, a shortest path needs to be accustomed with power system fundamental laws (10) and (11).

3.3. Shortest path resistance (R_{sh})

To deploy a metric for current flow analysis in AG assume that electrical power behaves as a discrete data packet and follows the shortest or the most efficient path between a source node (generator bus) to destination nodes (load bus). A R_{sh} from v_i to v_j is a finite sequence of nodes of L_G, satisfying v_i and $v_{i+1}, \in V$ for $i = 1, 2, 3, \ldots, N-1$ when line impedance, $Z \neq 0$. According to nearest node [21], the R_{sh} from a source node v_i to destination node v_j, described in the following manner considering ($v_i, v_j \in V$), and $i \neq j$

$$R_{sh} = \sum_{v_i, v_j \in V, i \neq j} Z_{ij}(v_i, v_{i+1}) \tag{12}$$

As given in (12) (R_{sh}) is defined as the sum of the weights of all adjacent edges (line impedance) associated with v_i to v_j which has to be a minimum path over all paths from node v_i to node v_j and satisfy the graph inequality ($R_{sh(v_i,v_j)} \leqslant R_{sh(v_i,v_n)} + R_{sh(v_j,v_n)}$). Power flow on transmission lines depends on its connectivity between pair of nodes(buses),hence, R_{sh} (12) will change with changes in network topology.

The geometrical concepts (3.1–3.3) have been used in formulation of proposed methodology.

4. Proposed methodology

To analyze changes in power flow on transmission line under normal to perturbed grid, we assumed grid topological data (offline) and real time current flow on transmission line (online PMU data) to be made available from WAMs, as shown in Fig. 6. The grid topological data of power network from WAMS offline data, contains the information of sparsely connected buses and transmission lines which is unable to describe entire grid connectivity. The concept of an AG has been used in the proposed methodology to analyze the impact of line tripping on geometry of current flow path using PFI and VI index.

4.1. Power Flow Index (PFI)

In a PG, each line has a protection relay to avoid damage due to line overloading. When a transmission line overloads, an over current relay intimates circuit breaker to trip the overloaded line. Tripping of one line may redistribute load among the neighboring lines which might overload other lines and initiate cascading. Hence, grid geometry will change the R_{eff} as well as $R_{sh(ij)}$ between a pair of vertices. In such a scenario, some performance index has to be defined which will measure the impact of changes in grid topology on current flow paths in AG. PFI analyse the line loading by means of geometry of current flow path in AG and help to classify underloaded and overloaded line in the grid. Formulation of

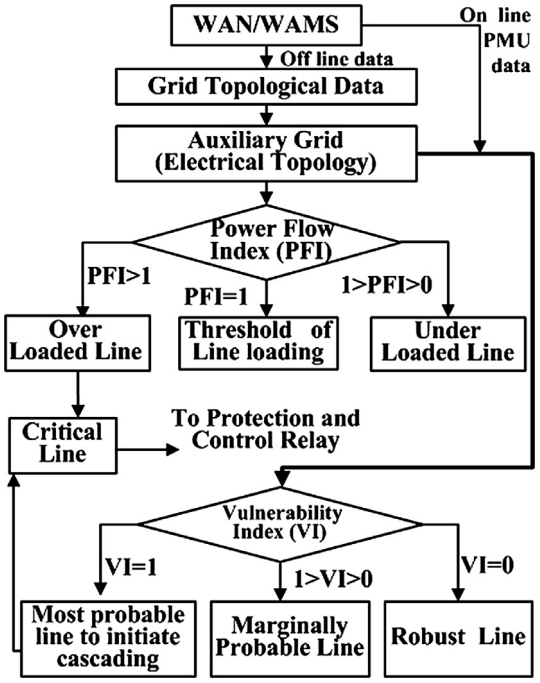

Fig. 6. Geometrical Framework: Flow diagram.

PFI is recognized from (11), (12) and [13]. PFI index is defined as a ratio of the $R_{eff(ij)}$ to $R_{sh(ij)}$ between the pair of vertices (buses) v_i and v_j.

$$PFI = \frac{R_{eff(ij)}}{R_{sh(ij)}} \tag{13}$$

PFI can be visualized by plotting a graph between power flow index verses transmission lines. Proposing this index allows in-depth analysis of current flow dynamics from normal to perturbed grid. According to (11)–(13) PFI can be interpreted as follows;

- Case 1- (PFI < 1): In this scale $R_{eff(ij)}$ is small, compared to $R_{sh(ij)}$ because there are many parallel paths which reduce the R_{eff} between pair of vertices v_i and v_j in AG. Hence, in case of line failure, current can follow alternate paths. Therefore, a power grid with more parallel paths, has a smaller R_{eff} resistance, and a relatively more robust power system against cascading failure. The lines belonging to this zone considered as underloaded lines.
- Case 2- (PFI $= 1$): This scale indicates that R_{eff} is equal to the analytical R_{sh} path. This scale determines the normal load flow limit or threshold of current flow path in AG. Hence, PFI equal to one is taken as threshold. Transmission lines with $1 \geqslant$ PFI > 0 is considered as underloaded lines.
- Case 3- (PFI > 1): In AG $R_{eff(ij)}$, increases with the decrease in the number of parallel paths (line outage) between pair of vertices v_i and v_j. Hence, PFI increases from threshold. PFI greater than one indicates increment in $R_{eff(ij)}$ in the perturbed grid. PFI scale in this case is considered as a local maxima scale which indicates the presence of overloaded lines in the network. Tripping of one line belongs to this scale may overload other lines, create stress in the power network, initiate cascading link failure, and may make the power system vulnerable.

PFI index helps in identifying underloaded and overloaded lines in the grid without using AC or DC load flow equations. The limitation of PFI is that, it does not quantify or measure vulnerability of

the system for imminent disturbances. It cannot predict probability of line tripping and location of critical line or vulnerability center of the grid with the knowledge of local graph connectivity. PFI index will not provide impact of line tripping (under PFI > 1) on system vulnerability. As (13) measures local connectivity or path distance not the entire grid connectivity or global path distance. To overcome these issues, vulnerability index (VI) has been defined to analyze line performance globally. This will also help in obtaining the location of the vulnerability center or network bottleneck.

4.2. Vulnerability Index (VI)

In the power transmission system (Fig. 1), supply and demand take place at buses (nodes), but overloading happens in the links. Hence, it is important to measure line overloading due to variation in any of the buses directly as well as indirectly (hidden) connected to that link. Probability of current flow on the line has been measured by the electric closeness between line and other nodes (Euclidean embedding around the line), which is defined as distance metric $d(v_i, v_j)$ in AG (L_0^+). The n dimensional Euclidean embedding defined in (14) and shown in Fig. 7 is a measure of electrical closeness between line v_{ij} and other nodes v_n in the AG.

$$d(v_i, v_j) = ((L_0^+)_{in} - (L_0^+)_{jn}) \tag{14}$$

The distance metric $d(v_i, v_j)$ geometrically measures n dimensional euclidean embedding around v_i, v_j. In (14) $n = 1, 2, 3, \ldots, N-1$ represents nodes (buses) in power grid or rows and columns of L_0^+ matrix (7). The mean of all n dimensional euclidean embedding (15) associated with the line $(v_i v_j)$ provides the information of the strongest electrical path distance with respect to the entire grid. Hence, the global path distance has been defined in (15).

$$M_{ij}(v_i v_j) = \frac{1}{(N-1)} \sum_{v_n} (d(v_i, v_j))_{jn} \tag{15}$$

The mean of euclidean embedding (distance metric) changes with change in physical topology. Any changes in physical topology will also change the electrical topology which will finally change the n dimensional euclidean embedding (14) and mean path distance (15) from the base case. To analyze the effect of topological changes on transmission lines robustness against vulnerability, the grid centrality (maximum embedding across the line) has been defined globally by replacing the $(R_{eff(ij)})$ of (13) by grid effective resistance or global distance metric (15) i.e. $M_{ij}(v_i v_j)$.

$$C_{ij}(v_i v_j) = \frac{1}{(N-1) R_{sh(ij)}} \sum_{v_n} (d(v_i, v_j))_{jn} \tag{16}$$

where C_{ij} measures the center of the grid robustness i.e. maximum embedding (alternate paths) in terms of global path distance $(d(v_i, v_j))_{jn}$ in AG.

Up to this point, changes in current flow path have been analyzed and measured purely on topological base. To incorporate line flow dynamics in vulnerability assessment, real power flow on the transmission line (online WAMS PMU data) has been taken into consideration. Multiplication of transmission line actual power

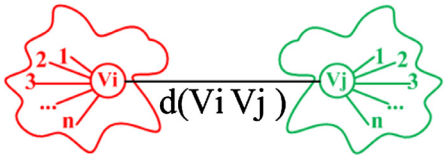

Fig. 7. Euclidean embedding in AG across v_i and v_j.

with graph centrality (16) will pinpoint the location of network centrality or robustness center again grid disturbances.

Hence, location of robust line against grid disturbances is measured by modifying (16) and (17).

$$C_{ij}(v_i v_j) = \frac{1}{(N-1) R_{sh(ij)}} \sum_{v_n} (d(v_i, v_j)_{jn})(P_{ij})(\rho_{ij}) \tag{17}$$

P_{ij} represents real transmission power on the line connected between a pair of vertices v_i and v_j. ρ is line vulnerability risk factor or tolerance against line fluctuation [5] Line vulnerability risk factor is assigned to each bus in the power grid as an operation risk factor, which represents the risk of experiencing power fluctuation in the bus. It is predefined to decide margin or tolerance limit against power fluctuations as. Eq. (17) defines the center of grid robustness. The generalized grid centrality can be measured as,

$$C_{ij}^{\text{nor}}(v_i, v_j) = \left[1 - \frac{C_{ij}(v_i, v_j)}{\max_{v_m v_k} C_{mk}(v_m v_k)}\right] \tag{18}$$

where m and k are the mth row and kth column vector of (L_0^+) matrix defining the line having maximum embedding within the same data sample. Eq. (17) provides global information of line connectivity whereas $C_{ij}^{\text{nor}}(v_i, v_j)$ in (18) provides the normalized grid centrality in the scale of zero to one. Evaluation of (18) provides the information of graph centrality or robustness against vulnerability in transmission system. Since grid vulnerability is the complementary of the robustness, vulnerability index can be defined as,

$$\text{VI} = 1 - C_{ij}^{\text{nor}}(v_i, v_j) \tag{19}$$

Vulnerability increases with the increase in VI. Higher value of VI indicates more variance from the mean (robustness center) or closeness towards vulnerability center or network bottleneck. The impact of line tripping on vulnerability in transmission system can be analyzed by VI index in the range of zero to one. VI analyze global path distance and reveals exactly where the bottleneck lies in the network. As shown in proposed model Fig. 6 and (19), VI metric has been defined as follows.

- Case 1: (VI = 0) It indicates the graph centrality or robust center (line) of the power network. Lines under this case are considered as robust lines. Tripping of robust line, power system can re-balanced without overloading any other element of the power network.
- Case 2: (1 > VI > 0) This scale measures the distance from grid robustness center and consider as a zone having marginally probable line to trip in the scenario of cascading. Tripping of line belonging to this zone may overload other lines.
- Case 3: (VI = 1) This case measures the maximum variance from the robustness center. This indicates the vulnerability center. Tripping of this line, several elements such as lines and transformers may become overloaded. The power system becomes unstable and may lead to cascade failure. Case 3 indicates the location of vulnerability center.

PFI and VI metrics proposed in this research work analyse line performance and identify dominant line in the normal to perturbed grid. Analysis of PFI and VI index, provides the information of local to global current flow path. A line is said to be critical when a local overload line becomes global vulnerability center.

Proposed mathematical model has been validated by simulation and also compared with our earlier probabilistic model. PFI and VI metrics used only the information of grid topology and the real power flow on transmission line. Mathematical modelling is validated by simulation in which analysis is carried-out from normal to perturbed grid. Disturbance initiated by tripping of one line

from the base case. The line utilization factor (LUF) has been used to select a maximum utilized line which can trip in the base case to initiate disturbances in PG as well as AG. The line utilization factor (LUF) [7] gives the information of utilization of individual line with respect to line capacity based on real time power flow on transmission line.

$$(\mathrm{LUF})_{ij} = \frac{P_{ij}}{T_{ij}^{c}} \tag{20}$$

where P_{ij} is the real power flow on transmission line and T_{ij}^{c} is the rated capacity of the transmission line ij.

5. Validation of proposed methodology

The proposed methodology, shown in Fig. 6, has been implemented on IEEE 30 bus test system using MATLAB and PowerWorld simulator. As shown in Fig. 8, IEEE 30 bus system [24] consists of 30 buses and 42 transmission lines consisting of 289.1-MW generation and 283.4-MW load flow capacity.

A topological model (Fig. 9) of IEEE 30 bus system under normal condition has been developed by allocating generator and load buses as vertex and transmission lines, transformers as edges. The numeric value across the link indicates the line impedance. For verification of the proposed metric, analysis of power flow has been carried out in two subsections. The first subsection considered as a base case where all transmission lines are working under their rated capacity. In the second subsection, vulnerability of power system has been analyzed under the successive line tripping. The probability of next tripping line has been identified by the VI index. A line is said to be critical with maximum PFI, and VI in the same sample. Cascading effect has been initiated by tripping of one line from the Base case of IEEE 30 bus system.

5.1. Base case analysis

At the base case, power flow on transmission lines considered under their rated capacity. PFI index V_s transmission line number is plotted in Fig. 10. According to PFI analysis (13), lines L21 and L40 carry more power and appeared in the local maxima zone. The VI index (19) for each line is calculated to identify the maximum loaded line in the grid. The VI graph of the base case is shown in Fig. 11. Calculated values of PFI and VI for some significant lines are shown in Table 1.

Analysis of PFI graph (Fig. 10) and Table 1, indicate that the lines under local maxima scale are lines L21 and L40. Analysis of VI index resolved that these lines are not critical lines because VI index of both the lines are 0.73 and 0.25, which is below one. Further, the line utilization factor (LUF) of lines L21 and L40, calculated from (20) and shown in Table 1 is 58% and 20% respectively. The LUF parameter of line L21 is 58% which is highest compared to other lines within the same sampled data. The vulnerability analysis for this sample instant shows that line L21 carries more power because its LUF is more but at the same time VI is below unity which indicates that the line L21 is not a critical line.

As shown in Fig. 11 and Table 1, line L29 has maximum VI, but this is not a critical line as it is not belong to the local maxima zone. The L29 identified as a healthy line is verified with the LUF of line L29 which is (18%) among all the lines. Hence, at the base case power flow on transmission lines are under there rated capacity. All the corresponding calculations for PFI, VI and LUF of some significant transmission lines are given in Table 1. The probabilistic analysis [8,9] of the IEEE 30 bus system base case data, also indicates normal Gaussian distribution at base case, which is shown in Fig. 18.

5.2. Analysis of cascading link failure

In this section PFI and VI measured under perturbed grid. Disturbances in the IEEE 30 bus system is created by tripping of a line from the base case. Probability of the next tripping line is considered as a line with maximum VI index. According to base case analysis from Table 1, line utilization or LUF of line L21 is 58%, which is highest compared to other lines. Hence line L21 has been tripped to initiate disturbances in the system.

Tripping of line L21 changed the grid topology, the R_{sh} (12), and the R_{eff} (11). The PFI corresponding to each line, is shown in Fig. 12 where lines L22, L29, L33 and line L40 comes under local maxima zone. The changes in the performance indices after tripping of line L21, are analyzed and summarized in Table 2 for some significant lines.

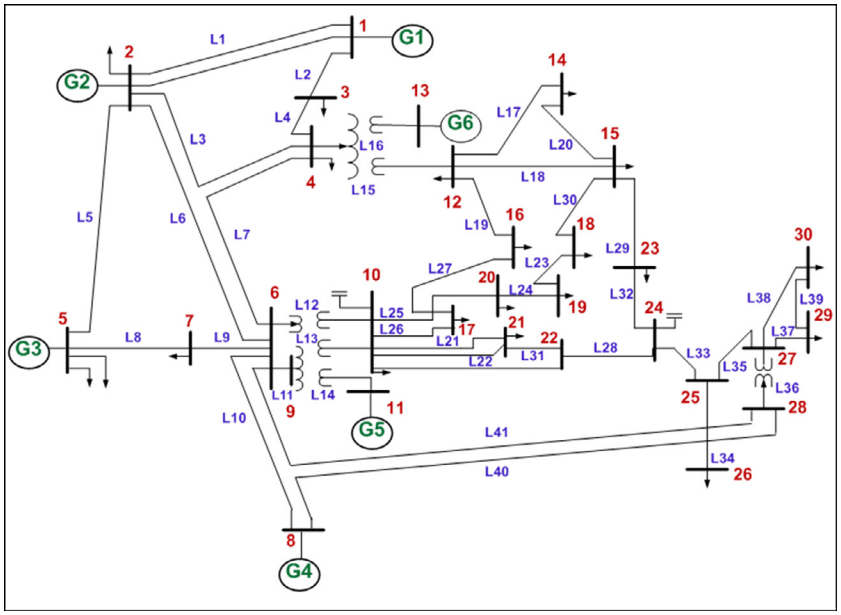

Fig. 8. One line diagram of IEEE 30 bus test power system.

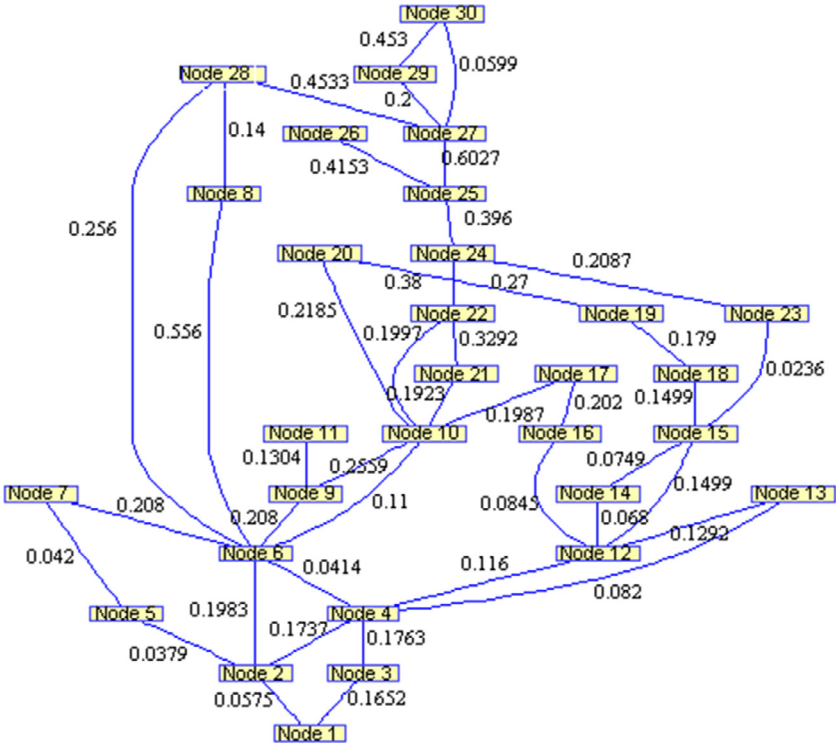

Fig. 9. Graphical representation of IEEE 30 bus power system.

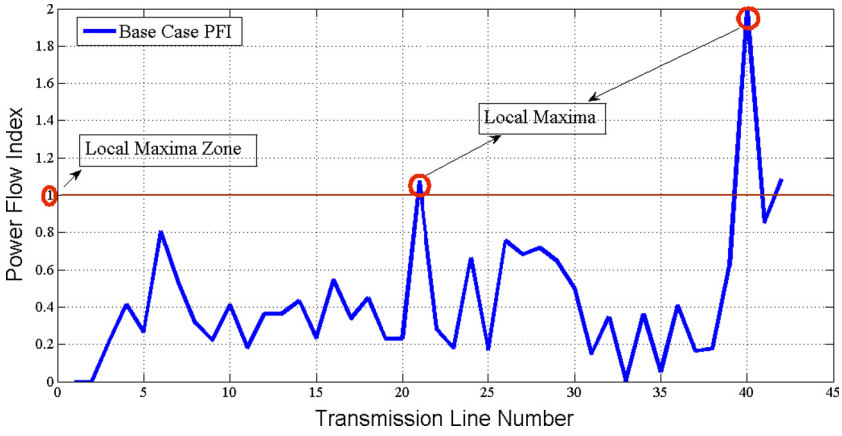

Fig. 10. PFI of transmission lines in IEEE 30 bus system at base case.

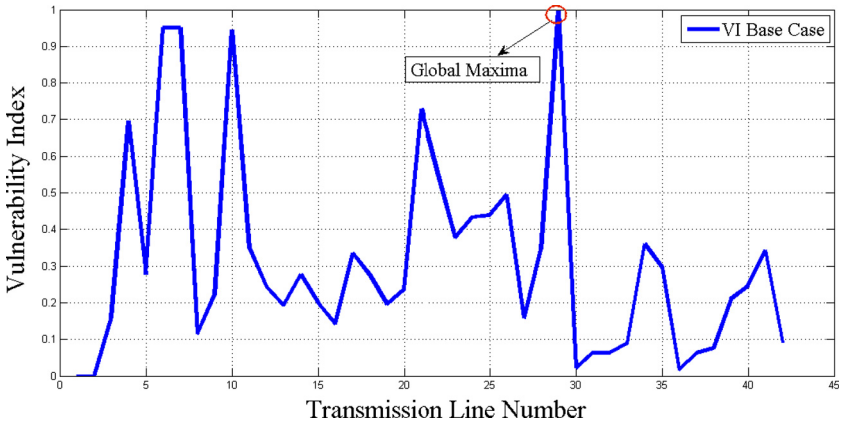

Fig. 11. VI Index of the IEEE 30 bus system at base case.

Table 1
Geometrical analysis of power flow at base case.

Line	R_{eff}	R_{sh}	PFI	C_{ij}^{nor}	VI	LUF (%)
L7	0.022	0.041	0.53	0.05	0.95	38.88
L10	0.017	0.042	0.41	0.06	0.94	45.62
L21	0.207	0.192	1.08	0.27	0.73	58.78
L29	0.020	0.023	0.64	0.0	1	18.13
L40	0.398	0.200	1.99	0.75	0.25	20

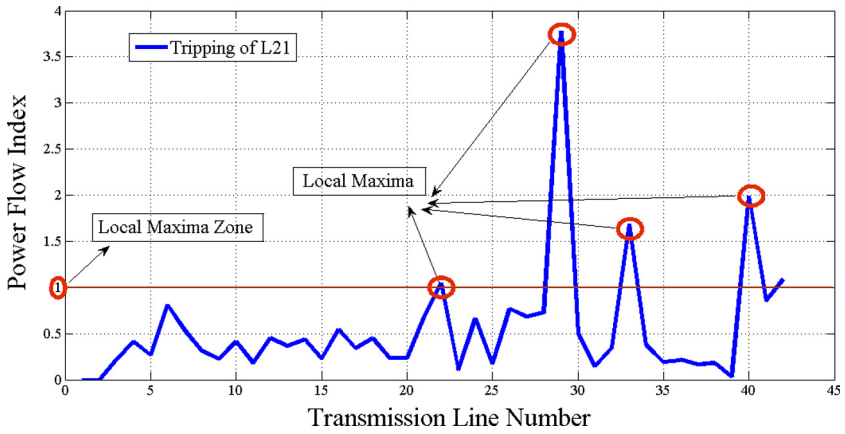

Fig. 12. PFI index after tripping of L21.

Table 2
Geometrical analysis of power flow after tripping of line L21.

Line.	R_{eff}	R_{sh}	PFI	C_{ij}^{nor}	VI	LUF (%)
L7	0.022	0.041	0.53	0.05	0.95	39
L22	0.180	0.171	1.05	0.0	1.0	77
L23	0.022	0.129	0.10	0.09	0.91	54
L29	0.089	0.023	3.78	0.88	0.12	20.3
L33	0.554	0.329	1.68	0.21	0.79	65
L40	0.398	0.200	1.99	0.63	0.37	30.5

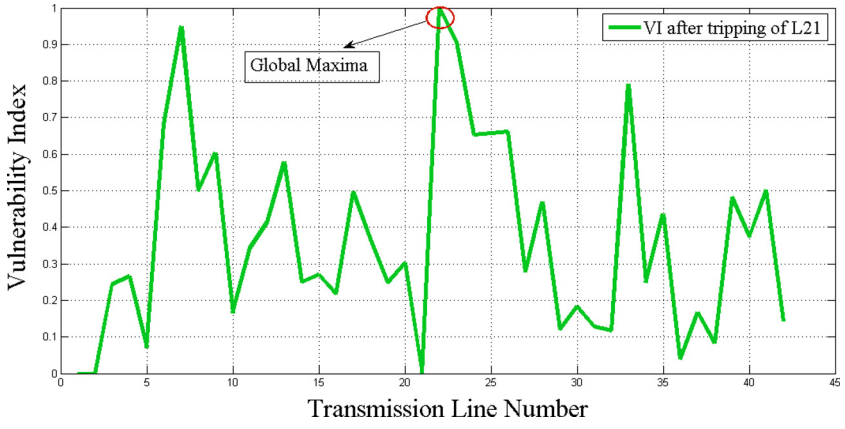

Fig. 13. VI index after tripping of L21.

Analysis of VI index from Fig. 13, indicate that the vulnerability center of the grid is located at line L22. The power grid vulnerability center identified by VI metric with PFI and LUF are shown in Table 2. VI of L22 is maximum (1) compared to other lines in the same data samples. Hence, according to proposed methodology, it is confirmed that the line L22 is the maximum stressed line and has the maximum probability to trip, in the scenario of cascading link failure. Though line L22 is identified as the most probable line to trip in the scenario of cascading link failure but it is not a critical line because its PFI value is not maximum among all the lines under the local maxima zone. As the cascading propagate, more stress is observed in the system, which is reflected in Fig. 14. Tripping of line L22 triggered many lines to enter into vulnerability zone and for some lines, the PFI index has drastically changed from normal zone to local maxima zone or visa-versa. This indicates stress in the power grid. The lines in the local maxima zone are shown by circle marks in Fig. 14. The corresponding PFI, VI, and LUF of some significant lines are calculated and shown in Table 3.

Under the stressed grid, as shown in VI graph of Fig. 15, VI is maximum at line L29. Also the PFI of line L29 is highest (11.67)

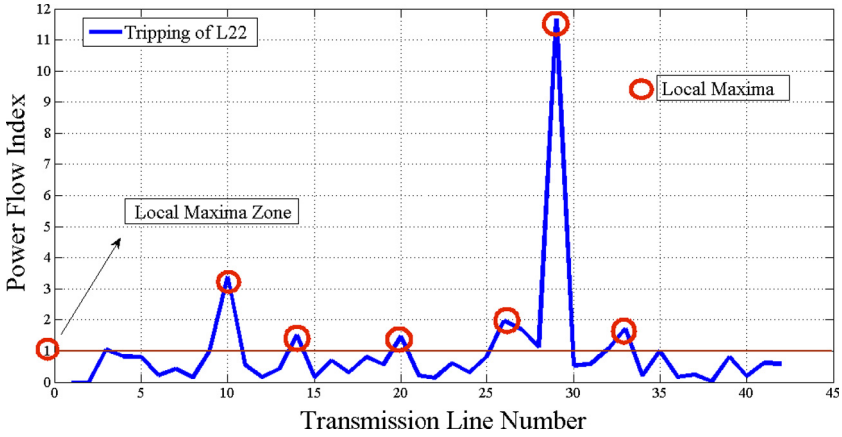

Fig. 14. PFI index after tripping of L22.

Table 3
Geometrical analysis of power flow after tripping of line L22.

Line	R_{eff}	R_{sh}	PFI	C_{ij}^{nor}	VI	LUF (%)
L10	0.142	0.042	3.39	0.94	0.06	20.86
L14	0.167	0.110	1.51	0.96	0.04	20
L20	0.294	0.199	1.47	0.94	0.06	53.75
L26	0.166	0.085	1.97	0.95	0.05	18.13
L27	0.127	0.075	1.69	0.05	0.95	29.38
L29	0.276	0.024	11.5	0.0	1	170
L33	0.567	0.329	1.72	0.76	0.24	65.2

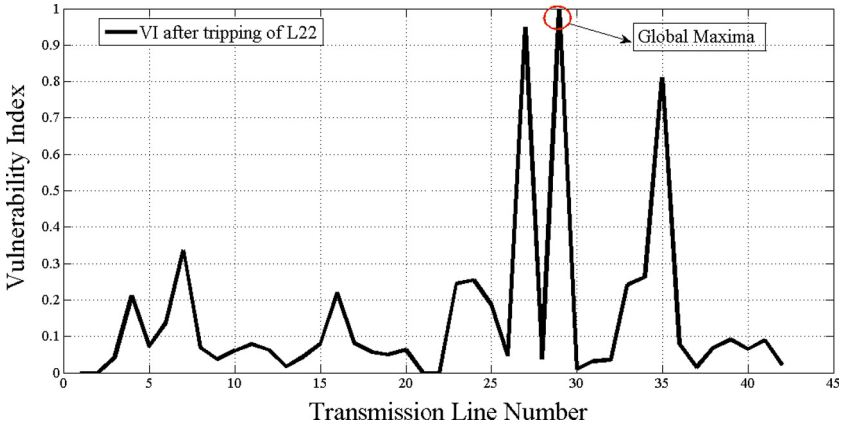

Fig. 15. VI index after tripping of L22.

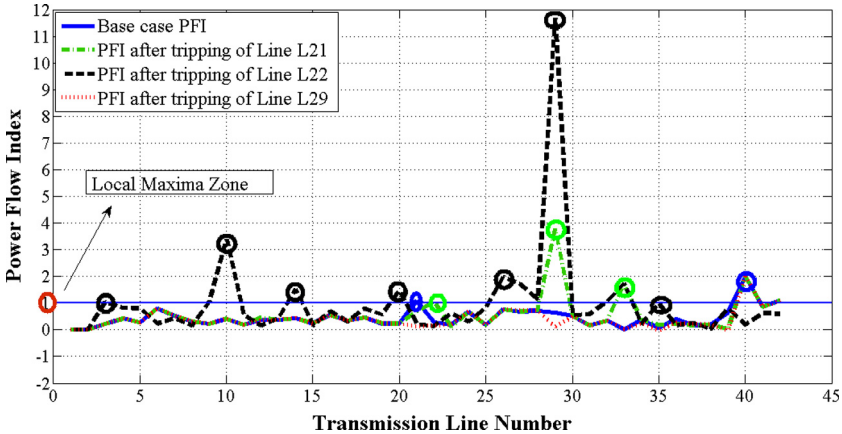

Fig. 16. PFI of normal to perturbed grid.

among all the local maxima lines. The cause of vulnerability i.e. line overloading has been checked by means of LUF index in Table 3. In Table 3, LUF of line L29 is 170%, which is maximum as compared to other lines. Analysis of this scenario indicates line L29 has maximum PFI, as well as maximum VI in the same sampled data set. As PFI as well as VI performance index is maximum at line L29, hence line L29 is identified as a critical line. The same line tripping sequence has been analyzed in our earlier probabilistic framework [9] in which system vulnerability was indicated by the changes in probability distribution curves from Gaussian to non Gaussian in terms of mean, variance, skewness and Kurtosis. As shown in probability distribution Fig. 18, at critical line the system parameters drastically increased i.e. skewness from 0.51 to 1.58. In the geometrical approach the same is reflected by increase in PFI from (3.78) to (11.67) and VI from 0.12 to 1 for line L29 compared to previous iteration (see Figs. 16 and 17).

Tripping of this critical line i.e. line L29 (Figs. 19 and 17) most likely results in the cascade failure. The same is verified on

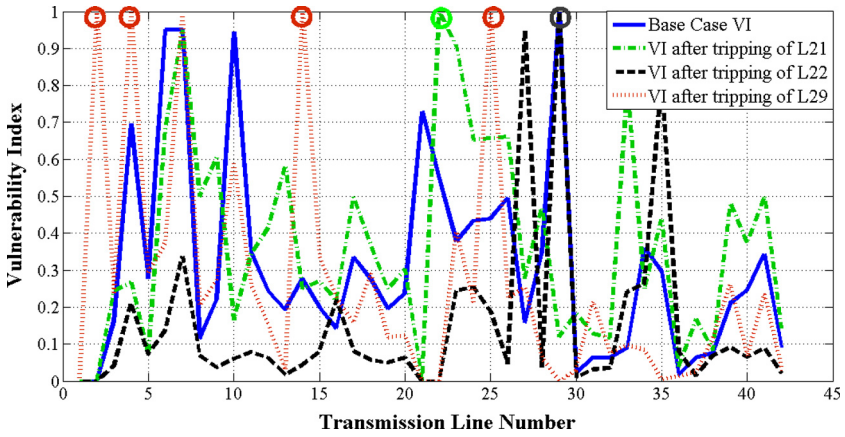

Fig. 17. VI of normal to pertirbed grid.

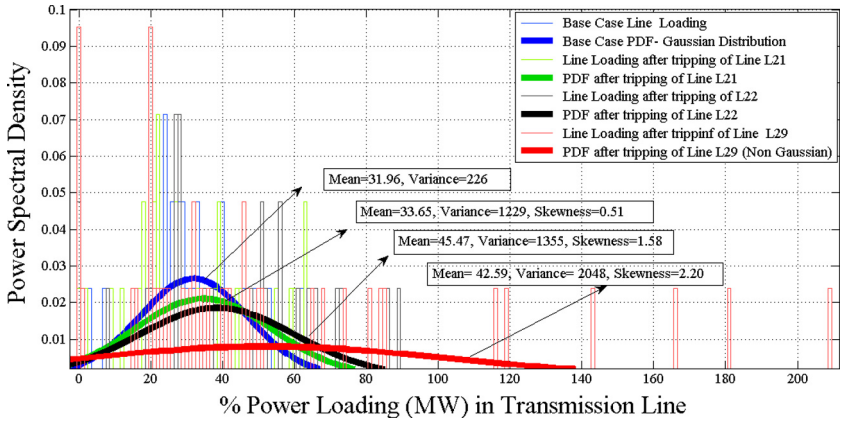

Fig. 18. Probabilistic Framework:PDF plots from normal to perturbed grid. *Source:* [9]

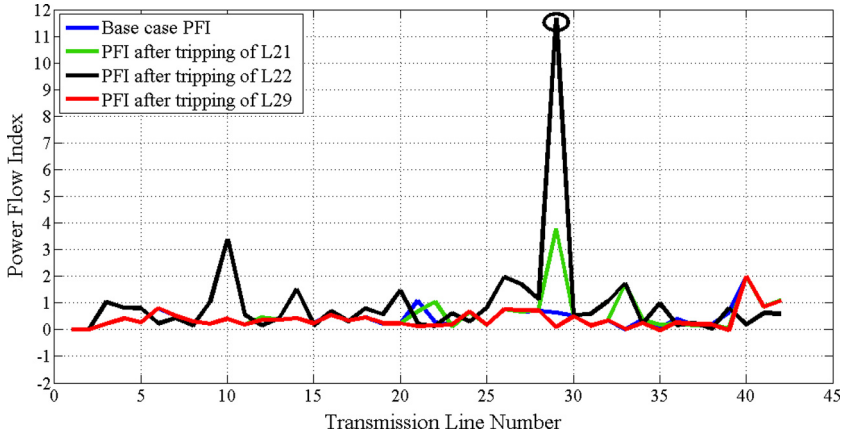

Fig. 19. Geometrical Framework: PFI index from normal to perturbed grid.

PowerWorld simulator, by tripping of line L29 in IEEE 30 bus system it resulted in blackout. Proposed PFI and VI indices derived from the topological data and the real time power flow on transmission line may be a good indicator for analysis and prediction of critical line in the perturbed power system.

5.3. Verification with probabilistic framework

Results of proposed geometrical framework for vulnerability analysis and identification of critical line has been verified with earlier probabilistic framework (Fig. 18). The same cascade link failure sequence in IEEE 30 bus system was analyzed in [9], using probabilistic load flow model. Wherein vulnerability in transmission line was measured from Gaussian to non Gaussian distribution which is shown in Fig. 18. In both the methodologies Figs. 18 and 19, 17 the critical line identified was the line L29. The red color PDF distribution curve in Fig. 18 highlights PDF of power flow after tripping of L29. The cumulative distribution function (CDF) approached one, and according to hypothesis testing, this scenario resulted in blackout. The proposed PFI and VI metrics have made it possible to physically observe the changes and predict critical line in power flow on transmission lines from normal to perturbed grid at the central monitoring station.

6. Conclusions

The hidden geometry of current flow path has been explored for analysis of vulnerability in power system. The defined PFI, and VI metrics helped to measure the impact of line tripping on load flow and identified the critical line in a perturbed grid. Tripping of critical line grid may lead to cascade failure. Early detection of critical link can help control system operator to judge the system abnormality and take corrective action. The proposed geometrical approach reduced computational complexity as it require only the grid topology and real power flow data. This methodology can be used to filter credible contingencies before performing a contingency analysis or to define control allocation to regulate power transfer over specific corridor. The PFI and VI index measures criticality of transmission lines which can be utilize in security assessment and centralized flow control in future smart grid wide area monitoring protection and control system.

Acknowledgement

The author would like to acknowledge the support of TEQIP-II through Center of Excellence in Complex and Non-Linear Dynamical Systems (CoE-CNDS), VJTI, Matunga Mumbai, India.

References

[1] Li Fangxing, Qiao Wei, Sun Hongbin, Wan Hui. Smart transmission grid: vision and framework. IEEE Trans Smart Grid 2010;1(2):168–77.
[2] Moslehi K, Kumar R. A Reliability perspective of the smart grid. IEEE Trans Smart Grid 2010;1(2):57–64.
[3] Liu X, Shahidehpour M, Cao Yijia, Li Zuyi, Tian Wei. Risk assessment in extreme events considering the reliability of protection systems. IEEE Trans Smart Grid 2015;6(2):1073–81.
[4] Mario A, Daniel S, Dilan J, Nedic Dusko P, Ron N. Value of security: modelling time-dependent phenomena and weather conditions. IEEE Trans Power Syst 2002;17(3):543–8.
[5] Sullivan RL, Lee R. Power system planning. New York, NY, USA: McGraw-Hill International Book Company; 1977.
[6] Galiana FD. Bond estimations of the severity of line outages in the power system contingency analysis and ranking. IEEE Trans Power Appar Syst 1984; PAS-103:2612–24.
[7] Wang XF, Song Y, Irving M. Modern power systems analysis. Springer-Verlag; 2008. 4York.
[8] Gupta SR, Kazi FS, Wagh SR, Singh NM. Probabilistic framework for evaluation of smart grid resilience of cascade failure. In: Innovative smart grid technologies. IEEE PES ISGT Asia, Kuala Lumpur, Malaysia; 20–23 May, 2014. p. 255–60.
[9] Gupta S, Kambli R, Wagh S, Kazi F. Support vector machine based proactive cascade prediction in Smart Grid using probabilistic framework. IEEE Trans Ind Electron 2015;62(4):2478–86.
[10] Dobson I, Carreras Benjamin, Lynch Vickie, Newman David. Complex systems analysis of series of blackouts: cascading failure, critical points, and self-organization. Chaos 2007;17(2):1–13.
[11] Pepyne D. Topology and cascading line outages in power grid. J Syst Sci Syst Eng 2007(June):202–21.
[12] Tate Joseph E, Overbye Thomas J. Line outage detection using phasor angle measurements. IEEE Trans Power Syst 2008;23(4):1643–51.
[13] Banirazi R, Jonckheere E. Geometry of power flow in negatively curved power grid. In: 49th IEEE conference on decision and control, Atlanta, GA, USA; December 15–17, 2010. p. 6259–64.
[14] De La Ree Jaime, Centono Virgilio, Thorp James S, Phadke AG. Synchronized phasor measurement applications in power systems. IEEE Trans Smart Grid 2010;1(1).
[15] Hauer JF, Bhatt NB, Shah K, Kolluri S. Performance of WAMS East in providing dynamic information for the North East blackout of August 14, 2003. In: Proc. IEEE PES general meeting, Denver, CO; 2004.
[16] Ricardo M, Alvaro T, George A, Rios Mario A. Sequential islanding of power systems as a security strategy. Int Rev Electr Eng (I.R.E.E.) 2011;6(7):3058–66.
[17] Ding L, Gonzalez-Longatt FM, Wall P. Two step spectral clustering controlled islanding algorithm. IEEE Trans Power Syst 2013;28:75–84.
[18] Sun K, Hur K, Zhang P. A new unified scheme for controlled power system separation using synchronized phasor measurements. IEEE Trans Power Syst 2011;26:1544–54.
[19] Teoman G, George G, Minghai L. Generalized line outage distribution factors. IEEE Trans Power Syst 2007;22(May):879–81.
[20] Mesbahi M, Egerstedt M. Graph theoretic methods in multiagent networks. Princeton University Press. eBook ISBN: 9781400835355.
[21] Johnson Donald B. Effective algorithms for shortest path in sparse networks. J ACM 1977;24(1):1–13.
[22] Barooah Prabir, Hespanha Joaop. Graph effective resistance and distributed control: spectral properties and applications. In: Proceedings of the 45th IEEE conference on decision and control, Manchester San Diego, CA, USA; December 13–14, 2006. p. 3479–85.
[23] Ellens W, Spieksma FM, Van Mieghemc P, Jamakovic A, Kooij RE. Effective graph resistance. J Linear Algebra Appl 2011;435(10):2491–506.
[24] Gnanadass R. Appendix – A Data for IEEE-30 Bus Test System; 2011. Available: <https://www.google.com/shodhganga.inflibnet.ac.in/bitstream/10603/1221/18/18_appendix.pdf>.